International Journal of Engineering, Mathematical and Physical Sciences
ISSN: 2517-9934
Vol:3, No:5, 2009

PeliGRIFF: a parallel DEM-DLM/FD method for DNS of particulate flows with collisions

Anthony Wachs [a], Guillaume Vinay [a], Gilles Ferrer [b], Jacques Kouakou [a], Calin Dan [a], Laurence Girolami [a]

Abstract—An original Direct Numerical Simulation (DNS) method to tackle the problem of particulate flows at moderate to high concentration and finite Reynolds number is presented. Our method is built on the framework established by Glowinski and his coworkers [1] in the sense that we use their Distributed Lagrange Multiplier/Fictitious Domain (DLM/FD) formulation and their operator-splitting idea but differs in the treatment of particle collisions. The novelty of our contribution relies on replacing the simple artificial repulsive force based collision model usually employed in the literature by an efficient Discrete Element Method (DEM) granular solver. The use of our DEM solver enables us to consider particles of arbitrary shape (at least convex) and to account for actual contacts, in the sense that particles actually touch each other, in contrast with the simple repulsive force based collision model. We recently upgraded our serial code, GRIFF [1] [2], to full MPI capabilities. Our new code, PeliGRIFF [2], is developed under the framework of the full MPI open source platform PELICANS [3]. The new MPI capabilities of PeliGRIFF open new perspectives in the study of particulate flows and significantly increase the number of particles that can be considered in a full DNS approach: O(100000) in 2D and O(10000) in 3D. Results on the 2D/3D sedimentation/fluidization of isometric polygonal/polyedral particles with collisions are presented.

Keywords—Particulate flow; Distributed Lagrange Multiplier/Fictitious Domain method; Discrete Element Method; Polygonal shape; Sedimentation; Distributed computing; MPI

I. Introduction

THE comprehension of solid/solid and fluid/solid interactions in moderately to highly concentrated particulate flows is of great interest from both fundamental and practical point of views. The hydrodynamics of such complex flows is still partially understood, even if the fluid phase exhibits simple Newtonian properties and the particles are monodisperse spheres (3D) or circular cylinders (2D). The primary reason for such a limited understanding is the fact that such processes involve phenomena at very different scales from the particle to the flow domain. The momentum transfer from the smallest scales like the interaction between two nearby particles to the largest ones evidenced by the formation of clusters of particles leads to tremendous alterations of flow dynamics. In such flows, the consideration of coupling between fluid flow and particles motion can not be ignored, otherwise significantly flawed modeling of the phenomenon would be developed. The range of industrial and scientific applications of particulate flows is quite broad : rock cuttings in drilling operation in mining and petroleum engineering, river sediment in environmental sciences, fluidized beds in chemical engineering, suspension flows in rheology, blood cells in biological engineering, ...

Here we are interested in the numerical simulation of particulate flows at moderate to high concentration and finite Reynolds number $\mathcal{R}e <= 500$. As the concentration of solid bodies suspended in the fluid exceeds more or less 5%, the probability of collision between particles increases dramatically. As a consequence, this requires the use of proper contact laws and a model (or numerical method) to handle the numerous multi-body collisions. Besides, as $\mathcal{R}e$ exceeds 1, the fluid and particle inertia can not be ignored anymore and need to be incorporated in the governing equations. This is definitively mandatory if one hopes to model properly the non-linear mechanisms controlling the migration and rotation of particles and lacking in Stokes flow. Our objective is to present an original approach based on the combined advantages of Distributed Lagrange Multiplier/Fictitious Domain (DLM/FD) method for fluid/solid interactions and Discrete Element Method (DEM) for multi-body solid collisions. Our method uses the DLM/FD formulation of Glowinski et al. [1] together with their operator-splitting idea to facilitates computations but here the collision step is handled by the DEM solver. Our DEM solver manages particles of arbitrary shape (at least convex) and various size. As two particles collide, the soft-sphere approach allows them to slightly overlap and

[a] Fluid Mechanics Department, IFP, 1 & 4 , avenue du Bois Preau, 92852 Rueil-Malmaison Cedex, France
[b] Solid Mechanics Department, IFP, 1 & 4 , avenue du Bois Preau, 92852 Rueil-Malmaison Cedex, France

[1]GRIFF stands for "GRains In Fluid Flow".

[2]PeliGRIFF stands for "Parallel Efficient LIbrary for GRains In Fluid Flow".

collision forces are calculated based on the overlapping region. In the overlapping region, to avoid that the conflicting rigid body motion constraints of the two particles concerned are forced at the same velocity node, in which case the problem would be overconstrained, we use the same strategy as the one suggested by Singh et al. [4] i.e. we impose the constraint of the particle the gravity center of which is closer to that node. We show that the computation of 2D/3D particulate flow with polygonal/polyedral particles and actual collisions does not bring about any trouble. The overall method keeps the strong and robust convergence properties of standard DLM/FD implementations.

The number of particles that can be reasonably simulated in a DNS approach appears to be a crucial matter of concern. Though DNS permits to get some deep insight in the fluid/solid interactions since the velocity and pressure fields are fully resolved around solid bodies, the computing time is prohibitive and in most serial implementations, a few hundreds (respectively thounsands) particles in 3D (respectively in 2D) is the attainable upper bound. Using their original DLM/FD method and a serial implementation, Glowinski et al. [5] reported in 2001 the simulation of the sedimentation of 6400 circular cylinders in 2D and the fluidization of 1204 spheres in 3D. Feng and Michaelides [6], in 2005, used their code Proteus and matched the same performances by simulating the settling of 1232 spheres thanks to an IB-LBM (Immersed Boundary - Lattice Boltzmann Method). In both these contributions, computations were performed with a serial code. Nevertheless, they showed the formation of large hydrodynamic recirculations that involve tens to hundreds of particles. In 2005, Uhlmann [7] implemented a similar IB method and studied the sedimentation of 1000 spherical particles in a periodic box with a full MPI implementation which enabled him to consider fine meshes, up to $512 \times 512 \times 1024$ grid nodes. Computations were run on 64 and 128 processors. With other kinds of approach where the flow is averagely solved, i.e., local averaging of physical properties on the fluid computational cell, a larger number of particles can be simulated. For instance, Tsuji et al. [8], [9] showed impressive results with up to 16million particles, but in their approach the fluid/solid interactions are not as precisely described as in a full DNS one like the DLM/FD or IB methods.

Being able to simulate a large number of particles is an objective in itself from the pure computational viewpoint but more importantly, it opens a new broad range of classes of problem that can be investigated with this type of approach. In other words, if in a given situation, experiments revealed that hydrodynamic structures involving thousands of particles manifest in the process and that the code used to simulate this phenomenon cannot handle more than a few hundreds, this situation can simply not be examined. In this perspective, a full MPI implementation on large distributed clusters is a real breakthrough.

Compared to our previous work [10], [11], [2], we present here our new code PeliGRIFF. This new version of our DEM-DLM/FD approach is full MPI and enables us to extend significantly the number of particles present in our systems. We illustrate the robust capabilities and satisfactory performances of PeliGRIFF on the 2D/3D sedimentation and fluidization of isometric polygonal/polyedral particles in a Newtonian with collisions.

II. Governing equations

Let Ω be a bounded domain of $\mathbb{R}^d$, $d \in < 2,3 >$ and $\partial\Omega$ its boundary. Suppose that Ω is filled with N_P rigid particles $P_i(t)$, $i \in < 1, N_P >$. For simplicity, we consider $N_P = 1$, the extension to the multi-body case being straightforward. Please note that we shall work with dimensionless quantities throughout the whole paper and distinghuish any dimensional quantities by a "star" symbol.

In the formulation below, we consider the case of mixed boundary conditions. Let us assume that $\partial\Omega$ can be sub-divided in Γ_0 and Γ_1 on which velocity $\boldsymbol{u}^*$ and pressure p^* fields satisfy:

$$\boldsymbol{u}^* = \boldsymbol{u}^*_{\Gamma_0} \; on \, \Gamma_0 \tag{1}$$

$$(2\eta^* \boldsymbol{D}^*(\boldsymbol{u}^*) - p^*)\boldsymbol{n}^* = \boldsymbol{g}^*_{\Gamma_1} \; on \, \Gamma_1 \tag{2}$$

where $\boldsymbol{n}^*$ is the unit outward normal vector to Γ_1, η^* the fluid viscosity and $D^* = \frac{1}{2}(\nabla \boldsymbol{u}^* + \nabla \boldsymbol{u}^{*t})$ the rate-of-strain tensor. Governing equations can be non-dimensionalized by introducing the following scales : L_c for length, U_c for velocity, L_c/U_c for time, $\rho^*_f U_c^2$ for pressure and $\rho^*_f U_c^2/L_c$ for rigid-body motion Lagrange multiplier. The variational combined momentum equations that govern both the fluid and solid motion reads [1]:

1) Combined momentum equations

$$\begin{aligned} &\int_\Omega \left(\frac{\partial \boldsymbol{u}}{\partial t} + \boldsymbol{u} \cdot \nabla \boldsymbol{u} \right) \cdot \boldsymbol{v} d\boldsymbol{x} - \int_\Omega p \nabla \cdot \boldsymbol{v} d\boldsymbol{x} \\ &+ \frac{1}{\mathcal{R}e_c} \int_\Omega 2\boldsymbol{D}(\boldsymbol{u}) : \boldsymbol{D}(\boldsymbol{v}) d\boldsymbol{x} \\ &+ \int_{P(t)} \boldsymbol{\lambda} \cdot \boldsymbol{v} d\boldsymbol{x} = \int_{\Gamma_1} \boldsymbol{g}_{\Gamma_1} \cdot \boldsymbol{v} d\Gamma, \quad \forall \boldsymbol{v} \in \mathcal{V}_0(\Omega) \end{aligned} \tag{3}$$

$$(\rho_r - 1)\left[V_P\left(\frac{\partial \boldsymbol{U}}{\partial t} - Fr\frac{\boldsymbol{g}^*}{g^*}\right)\cdot \boldsymbol{V} + \left(\boldsymbol{I}_P\frac{\partial \boldsymbol{\omega}}{\partial t} + \boldsymbol{\omega}\times\boldsymbol{I}_P\cdot\boldsymbol{\omega}\right)\cdot\boldsymbol{\xi}\right] - \sum_j \boldsymbol{F}_{cj}\cdot\boldsymbol{V} - \sum_j \boldsymbol{F}_{cj}\cdot\boldsymbol{\xi}\times\boldsymbol{R}_j - \int_{P(t)}\boldsymbol{\lambda}\cdot(\boldsymbol{V}+\boldsymbol{\xi}\times\boldsymbol{r})d\boldsymbol{x} = \boldsymbol{0},\ \boldsymbol{V}\in\mathbb{R}^d,\ \boldsymbol{\xi}\in\mathbb{R}^{\tilde{d}} \quad (4)$$

$$\int_{P(t)}\boldsymbol{\alpha}\cdot(\boldsymbol{u} - (\boldsymbol{U}+\boldsymbol{\omega}\times\boldsymbol{r})d\boldsymbol{x} = 0, \quad \forall\boldsymbol{\alpha}\in\Lambda(t) \quad (5)$$

2) Continuity equation

$$-\int_\Omega q\nabla\cdot\boldsymbol{u}d\boldsymbol{x} = 0, \quad \forall q\in\mathcal{P}_0(\Omega) \quad (6)$$

where $\boldsymbol{u}\in\mathcal{V}_{\Gamma_0}(\Omega)$, $p\in\mathcal{P}_{\Gamma_1}(\Omega)$, $\boldsymbol{\lambda}\in\Lambda(t)$ denotes the distributed Lagrange multiplier vector, $\boldsymbol{U}\in\mathbb{R}^d$ the particle translational velocity vector, $\boldsymbol{\omega}\in\mathbb{R}^{\tilde{d}}$ the particle angular velocity vector, $\tilde{d}$ the number of non-zero components of $\boldsymbol{\omega}$ (if $d=2$, $\boldsymbol{\omega}=(0,0,\omega_z)$ and $\tilde{d}=1$, else $\tilde{d}=d$), $(\boldsymbol{v},q,\boldsymbol{\alpha},\boldsymbol{V},\boldsymbol{\xi})$ the test functions for $(\boldsymbol{u},p,\boldsymbol{\lambda},\boldsymbol{U},\boldsymbol{\omega})$ respectively, $\boldsymbol{F}_{cj}\in\mathbb{R}^d$ the contact forces, $\boldsymbol{R}_j\in\mathbb{R}^d$ the vectors between particle gravity center and contact point, $\boldsymbol{r}$ the position vector with respect to particle gravity center, $V_P = M^*/(\rho_s^* L_c^d)\in\mathbb{R}$ the dimensionless particle volume, M^* the particle mass, $\boldsymbol{I}_P = \boldsymbol{I}_P^*/(\rho_s^* L_c^{d+2})\in\mathbb{R}^{\tilde{d}\times\tilde{d}}$ the dimensionless particle inertia tensor, $\rho_s^*\in\mathbb{R}$ the particle density, $\boldsymbol{g}^*\in\mathbb{R}^d$ the gravity acceleration, $g^*\in\mathbb{R}$ the gravity acceleration modulus, $\mathcal{R}e_c = \frac{\rho_f^* U_c L_c}{\eta^*}$ the Reynolds number, $Fr = \frac{g^* L_c}{U_c^2}$ the Froude number and $\rho_r = \frac{\rho_s^*}{\rho_f^*}$ the density ratio.

In equations above, we have introduced the following functional spaces:

$$\mathcal{V}_0(\Omega) = \{\boldsymbol{v}\in\mathcal{H}^1(\Omega)^d | \boldsymbol{v} = 0\ on\ \Gamma_0\} \quad (7)$$

$$\mathcal{V}_{\Gamma_0}(\Omega) = \{\boldsymbol{v}\in\mathcal{H}^1(\Omega)^d | \boldsymbol{v} = \boldsymbol{u}_{\Gamma_0}\ on\ \Gamma_0\} \quad (8)$$

$$\mathcal{L}_0^2(\Omega) = \{q\in\mathcal{L}^2(\Omega) | \int_\Omega q d\boldsymbol{x} = 0\} \quad (9)$$

$$\mathcal{P}_0(\Omega) = \{q\in\mathcal{L}_0^2(\Omega) | q = 0\ on\ \Gamma_1\} \quad (10)$$

$$\mathcal{P}_{\Gamma_1}(\Omega) = \{q\in\mathcal{L}_0^2(\Omega) | q = p_{\Gamma_1},\ \boldsymbol{g}_{\Gamma_1} = -p_{\Gamma_1}\boldsymbol{n}\ on\ \Gamma_1\} \quad (11)$$

$$\Lambda(t) = \mathcal{H}^1(P(t))^d \quad (12)$$

III. Collision model: DEM solver

Binary hard sphere model and soft sphere model are the two categories of collision model for particulate flows [12]. For the hard sphere model, the momentum exchange between two colliding particles takes place exactly at the time when the two particles touch. In contrast, for the soft sphere model, the velocity of colliding particles is determined from Newton's equations of motion with collision forces of soft potential being a function of separation or overlap distances between particles and possibly particles velocity [13], [14], as shown in Figure 1. In our DEM granular solver, the considered collision forces comprise:

- an elastic restoring force

$$\boldsymbol{f}_{el} = k_n\delta_{ij}\boldsymbol{n} \quad (13)$$

where k_n denotes the normal contact stiffness, δ_{ij} the overlapping distance between particles i and j and $\boldsymbol{n}$ the unit normal vector pointing between particles i and j gravity centers.

- a viscous dynamic force

$$\boldsymbol{f}_{dn} = -2\gamma_n m_{ij}\boldsymbol{U}_{rn} \quad (14)$$

in the normal direction to account for the dissipative aspect of the contact, where γ_n is the normal dynamic friction coefficient, $m_{ij} = \frac{M_i M_j}{M_i+M_j}$ the reduced mass of particles i and j and $\boldsymbol{U}_{rn}$ the normal relative velocity between particles i and j.

- a tangential friction force

$$\boldsymbol{f}_t = -min\{\mu_c|\boldsymbol{f}_{el}|, |\boldsymbol{f}_{dt}+\boldsymbol{f}_s|\}\boldsymbol{t} \quad (15)$$

$$\boldsymbol{f}_{dt} = -2\gamma_t m_{ij}\boldsymbol{U}_{rt} \quad (16)$$

$$\boldsymbol{f}_s = -k_s\int_0^{t_c}\boldsymbol{U}_{rt}dt \quad (17)$$

where $\boldsymbol{f}_{dt}$ denotes the dissipative frictional contribution, γ_t the dissipative tangential friction coefficient, $\boldsymbol{U}_{rn}$ the tangential relative velocity between particles i and j, $\boldsymbol{f}_s$ the static frictional contribution which behaves like an incremental spring that stores energy during the time of contact t_c and k_s the static friction coefficient. Note that the magnitude of the tangential friction force is limited by the Coulomb frictional limit calculated with the Coulomb dynamic friction coefficient μ_c.

The total collision force acting on a particle i is the sum of contributions related to the contact with neighbouring particles j :

$$\boldsymbol{F}_{ci} = \sum_j \boldsymbol{F}_{cij} = \sum_j(\boldsymbol{f}_{el}+\boldsymbol{f}_{dn}+\boldsymbol{f}_t)_{ij} \quad (18)$$

IV. Computational features

Details about the features of our numerical and computational approach can be found in our last contribution to the literature [2]. For the sake of conciseness, we merely sum up below the main ingredients of our strategy:

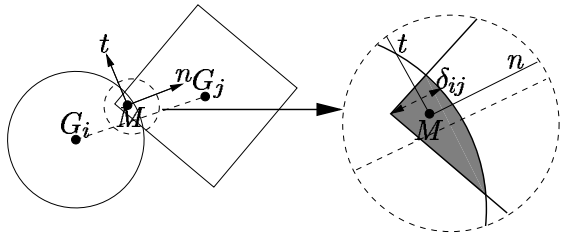

Fig. 1: Contact between two particles: G_i and G_j denote gravity center of particles i and j respectively, M the contact point, n and t unit normal and tangential vectors at the contact point respectively and δ_{ij} the overlapping distance

- the solving algorithm is based on operator-splitting techniques, i.e. at each time step we solve the following sequence of sub-problems:
  1) a degenerated Stokes problem to impose incompressibility (divergence free of velocity field) solved by an Uzawa/PCG (preconditioned conjugate gradient) iterative procedure,
  2) a purely advection problem treated by a Taylor-Galerkin wave-like method,
  3) a purely diffusive (viscous) problem solved by a PCG iterative procedure,
  4) a purely granular problem to predict particles velocity and position
  5) a DLM/FD problem to account for fluid/solid interactions solved by an Uzawa/PCG iterative procedure to correct particles and fluid velocity,
  6) a purely granular problem to correct particles position (and possibly velocity in case of further collisions).

  Compared to [2], we add the correction step 6, as suggested by Glowinski [1] and used by us in [10], [11].
- the spatial discretization is of the Finite Element type with triangular P1isoP2/P1 (Pironneau-Bercovier) and tetraedral P2/P1 (Taylor-Hood) elements for the velocity and pressure fields in 2D and 3D respectively.
- the spatial discretization of the distributed Lagrange multiplier field is based on the collocation-point method that assumes that each particle is cover by a set of points on which the test functions are Dirac measures [1], [2]. A special treatment is necessary as two particles collide (see [2] for more details). Figure 2 illustrates the set of points of two colliding circular cylinders in 2D.
- the granular sub-problem is solved by a second-order accurate leap-frog scheme and a highly efficient linked-cell algorithm is employed to detect particle collisions [15].
- the fluid solver is parallelized with classical domain decomposition technique implemented in PELICANS platform with open source PETSc library for all matrix operations.
- the granular solver runs in serial mode but its computational cost never exceeds more than 5% of the whole computing time. The specific MPI communications implemented in the DLM/FD problem consists of reduction and broadcast to and from the master process on which the granular solver runs and all other processes. This temporary solution (prior to the parallelization of the granular solver) shows good computational and satisfactory scalability properties.

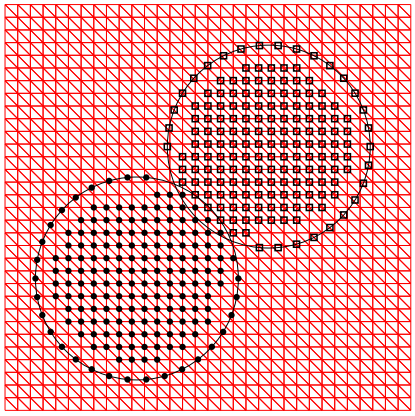

Fig. 2: DLM/FD set of points for two colliding circular particles

V. Results

We illustrate here the robust capabilities of PeliGRIFF on the effect of particle shape in sedimentation and fluidization problems. Additional results beyond the ones shown below will be presented during our oral presentation at the conference (including movies to highlight the dynamic feature of this type of flows). In the paper here, we restrict the number of particles to $O(1000)$ for clarity purposes in figures.

In the sedimentation problem, the motion of solid bodies is driven by the density difference with the fluid. The issue of chosing scales of velocity U_c and length L_c to non-dimensionalize results is not straightforward. Since in all cases considered in this paper inertia is non-negligible, we suggest to estimate U_c based on a balance between inertia and buoyancy [16], [2]. We chose for all

particle shapes $L_c = D_e^*$, where D_e^* is the diameter of a circular cylinder (respectively sphere) having the same surface (respectively volume) as the particle. Therefore, we have:

$$\text{in 2D}: \quad \frac{\rho_f^* D_e^* U_{c0}^2}{2} = \frac{\pi D_e^{*2}}{4}(\rho_s^* - \rho_f^*)g^*$$
$$\Rightarrow \quad U_{c0} = \sqrt{\frac{\pi D_e^*}{2}\frac{\rho_s^* - \rho_f^*}{\rho_f^*}g^*} \tag{19}$$

$$\text{in 3D}: \quad \frac{\rho_f^* \pi D_e^{*2} U_{c0}^2}{8} = \frac{\pi D_e^{*3}}{6}(\rho_s^* - \rho_f^*)g^*$$
$$\Rightarrow \quad U_{c0} = \sqrt{\frac{4D_e^*}{3}\frac{\rho_s^* - \rho_f^*}{\rho_f^*}g^*} \tag{20}$$

For multi-body sedimentation problems, we correct the velocity scale U_c by the Richardson-Zaki law for hindered settling and thus we get:

$$U_c = U_{c0}(1-\phi)^5 \tag{21}$$

where ϕ is the solid surface/volume fraction.

The first situation refers to the settling of a single particle in a plane infinite channel. The ratio between the channel width and the particle diameter is set to 4. We consider three isometric particle shapes: an ideal circular cylinder, a square and a triangle. Figure 3 presents the vorticity contours at relatively high Reynolds numbers $\mathcal{R}e$ (between 350 and 500) for the three different shapes. Since in all cases, $\mathcal{R}e$ is far above the critical Von Karmann transition $\mathcal{R}e_c \simeq 45-50$, the flow is clearly in the vortex shedding regime. Whereas the ideal circular cylinder periodicially oscillates with respect to the channel vertical symmetry plane and sheds alternate vortices, the coupling of hydrodynamic instabilities with the particle momentum transfer between translational to rotational motion leads to an almost chaotic trajectory of the two angular particles. The transition to organized chaos is even more noticeable in the case of the triangle.

The second situation pertains to the collective behavior of 300 triangles settling in a closed rectangular box at low $\mathcal{R}e \simeq 4$. The corresponding solid surface fraction is 20%. The initial particles pattern is randomly homogeneous. The computation is performed up to the point when all particles have settled to the bottom of the box. The dimensionless time-step and grid size employed in this simulation are $\Delta t = 2.10^{-3}$ and $h = 1/16$, which implies that 16 collocation points are used over the diameter of each particle. Around 30 000 time steps are required to simulate the whole sedimentation process. This computation was performed in serial mode for a total computing time of approximately 48 hours. Here

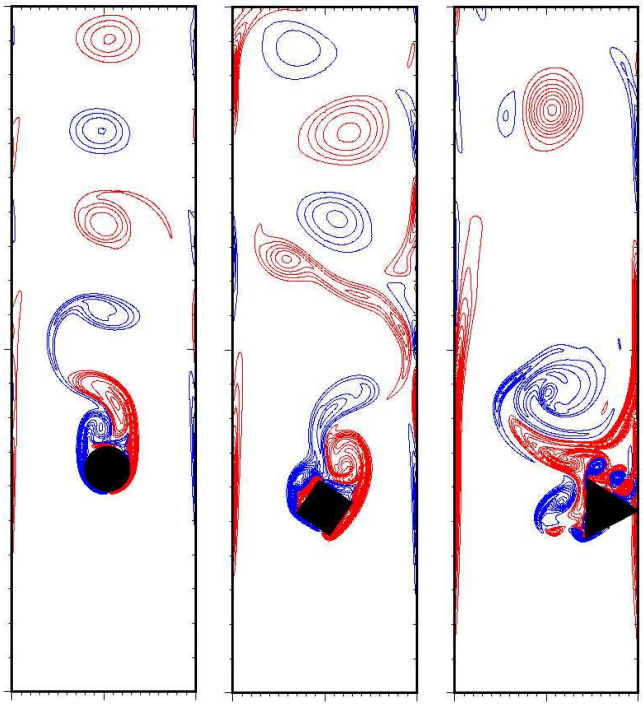

Fig. 3: Vorticity contours for a single particle settling in an infinite channel at $\mathcal{R}e \in [350:500]$: effect of particle shape, transition from periodic flow (circular cylinder) to organized chaos (triangle)

the numerous multi-body collisions occuring during the sedimentation process are properly handled by the DEM solver. In particular, the modelling of the packing of angular particles did not cause any difficulty, as exhibited in Figure 4-$t = 45.6$.

The third situation concerns the settling of 1528 isometric particles in a 3D closed cuboid box at $\mathcal{R}e \simeq 15$. As in the 2D case, at initial time, particles are randomly and homogeneously set in the domain and the solid volume fraction is 20%. The mesh comprises $\simeq 1.5$million finite elements, $\simeq 270000$ degree-of-freedom (dof) of pressure and $\simeq 6.0$million dof of velocity. The dimensionless time-step and grid size employed in this simulation are $\Delta t = 3.10^{-3}$ and $h = 1/10$, which implies that 10 collocation points are used over the diameter of each particle. Around 10 000 time steps are required to simulate the whole sedimentation process. This computation was performed in distributed mode on 32 AMD Barcelona 2.3Ghz processors of a Linux Cluster in 64bits for a total computing time of approximately 96 hours, i.e. 4 days. We illustrate the particle pattern together with iso-contours of settling velocity in 3 cutplanes for both the case of spherical

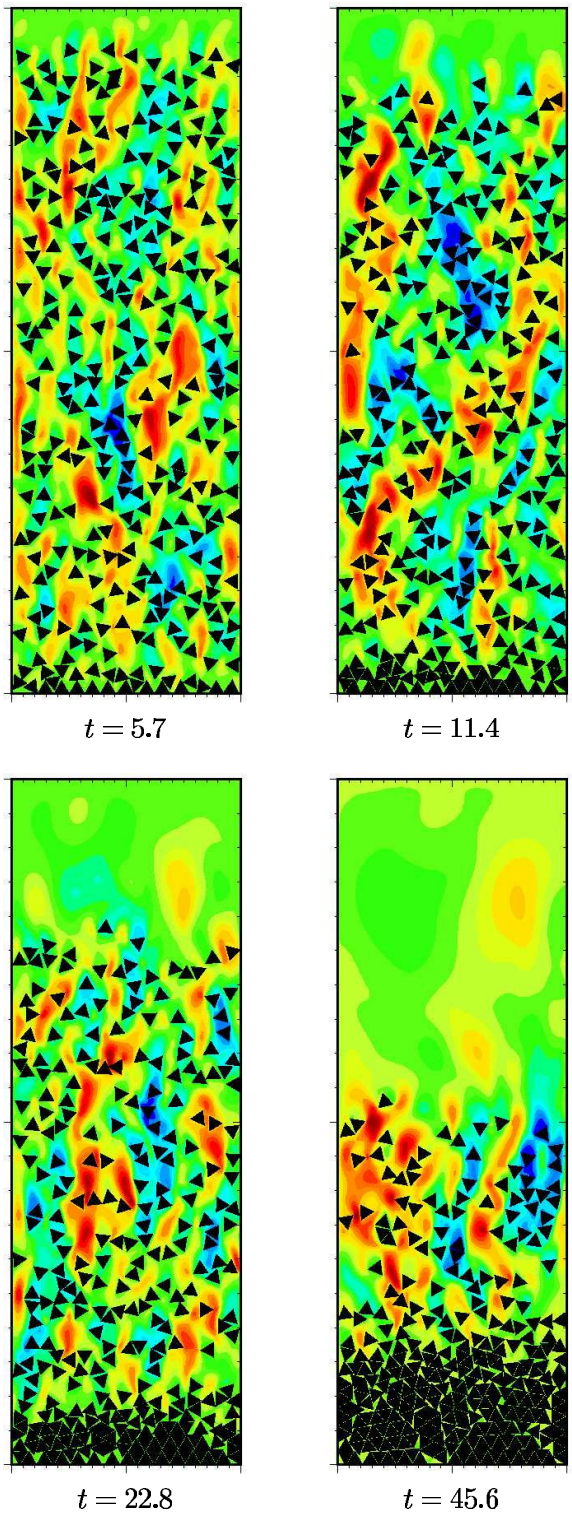

Fig. 4: Sedimentation of 300 triangles in a closed box at $\mathcal{R}e \simeq 4$, starting from an initial homogeneous layout: particles pattern with vertical velocity contours

and cubic particles. Let us mention that the simulation of 3D angular particles settling in a fluid has, to the best of our knowledge, never been reported in the literature such that it is fair to say that this result is truely novel.

VI. Conclusion and Perspectives

We proposed a new DNS approach to study particulate flows with collisions based on a DLM/FD formulation for fluid /solid interactions and a DEM method for solid/solid interactions. We showed that our code highlights a great potential to study a large range of particulate flows and to address the effect of particle shape. Thanks to our parallel implementation, our new code, PeliGRIFF, is able to manage a large collection of particles and permits to extend the current capabilities reported in the literature in the field of DNS of particulate flows by almost a decade (in 3D from $O(1000)$ to $O(10000)$).

References

[1] R. Glowinski, T.W. Pan, T.I. Hesla, and D.D. Joseph. A Distributed Lagrange Multiplier/Fictitious Domain method for particulate flow. *International Journal of Multiphase Flow*, 25:755–794, 1999.

[2] A. Wachs. A DEM-DLM/FD method for direct numerical simulation of particulate flows: sedimentation of polygonal isometric particles in a Newtonian fluid with collisions. *in press in Computers and Fluids*, 2009.

[3] *PELICANS, https://gforge.irsn.fr/gf/project/pelicans/*, 2008.

[4] P. Singh, T.I. Hesla, and D.D. Joseph. Distributed lagrange multiplier method for particulate flows with collisions. *International Journal of Multiphase Flow*, 29:495–509, 2003.

[5] R. Glowinski, T.W. Pan, T.I. Hesla, D.D. Joseph, and J. Periaux. A fictitious domain approach to the direct numerical simulation of incompressible viscous flow past moving rigid bodies: application to particulate flow. *Journal of Computational Physics*, 169:363–426, 2001.

[6] Z.G. Feng and E.E. Michaelides. Proteus: a direct forcing method in the simulations of particulate flows. *Journal of Computational Physics*, 202:20–51, 2005.

[7] M. Uhlmann. An immersed boundary method with direct forcing for the simulation of particulate flows. *Journal of Computational Physics*, 209:448–476, 2005.

[8] T. Tsuji, K. Yabumoto, and T. Tanaka. Spontaneous structures in three-dimensional bubbling gas-fluidized bed by parallel DEM-CFD coupling simulation. *in press in Powder Technology*, 2009.

[9] T. Tsuji, A. Ito, and T. Tanaka. Multi-scale structure of clustering particles. *Powder Technology*, 179(3):115–125, 2008.

[10] Z. Yu, X. Shao, and A. Wachs. A fictitious domain method for particulate flows with heat transfer. *Journal of Computational Physics*, 217(2):424–452, 2006.

[11] Z. Yu and A. Wachs. A fictitious domain method for dynamic simulation of particle sedimentation in Bingham fluids. *Journal of Non-Newtonian Fluid Mechanics*, 145(2-3):78–91, 2007.

[12] C. Crowe, M. Sommerfeld, and Y. Tsuji. *Multiphase flows with droplets and particles*. CRC press, 1998.

[13] P.A. Cundall and O.D.L. Strack. A discrete numerical model for granular assemblies. *Geotechnique*, 29:47–65, 1979.

[14] C.Y. Wu and A.C.F. Cocks. Numerical and experimental investigations of the flow of powder into a confined space. *Mech. of Materials*, 38:304–324, 2006.

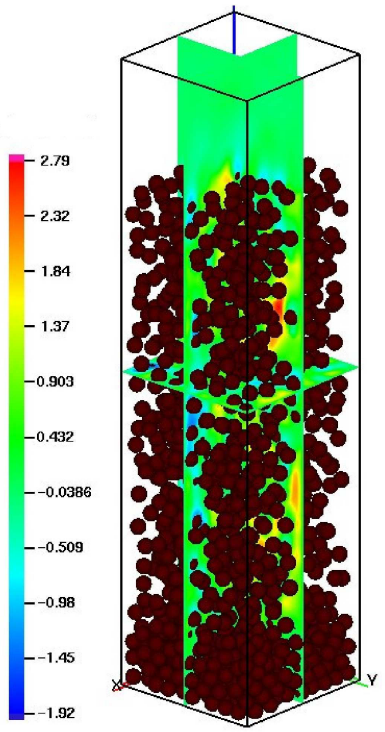

Spheres at $t = 11.7$

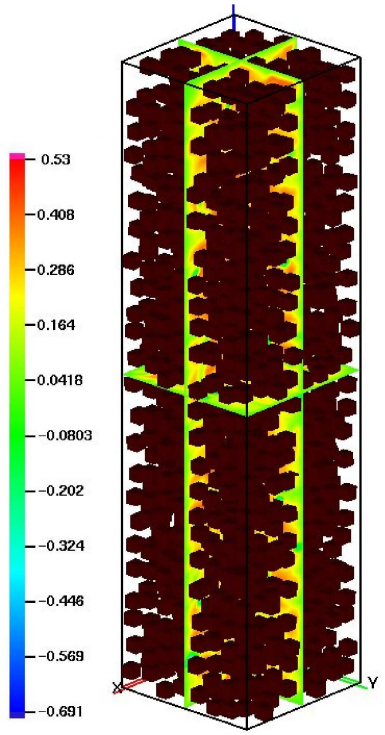

Cubes at $t = 0.3$

Fig. 5: Sedimentation of 1528 particles in a closed box at $\mathcal{R}e \simeq 15$, starting from an initial homogeneous layout: particles pattern with vertical velocity contours

[15] V. Komiwes, P. Mege, Y. Meimon, and H. Herrmann. Simulation of granular flow in a fluid applied to sedimentation. *Granular Matter*, 8:41–54, 2006.

[16] Z. Yu, N. Phan-Thien, Y. Fan, and R.I. Tanner. Viscoelastic mobility problem of a system of particles. *Journal of Non Newtonian Fluid Mechanics*, 104:87–124, 2002.

ACKNOWLEDGMENT

The authors wish to thank the PELICANS team, Cadarache, France, for their constant support and invaluable advices in the development of the parallel code PeliGRIFF.